A daganatos sejtek proliferációja és tumor növekedés

A daganat növekedését meghatározó tényezők

- Sejtciklus idő
- Proliferálódó sejtek aránya
- Sejtveszteség

A daganat térfogatának nyomon követése

- Rtg
- CT
- MRI
- Calliper

$V = \pi / 6 \times \text{átlagos átmérő}^3$

$V = 0{,}5 \times \text{hossz} \times \text{szélesség}^2$

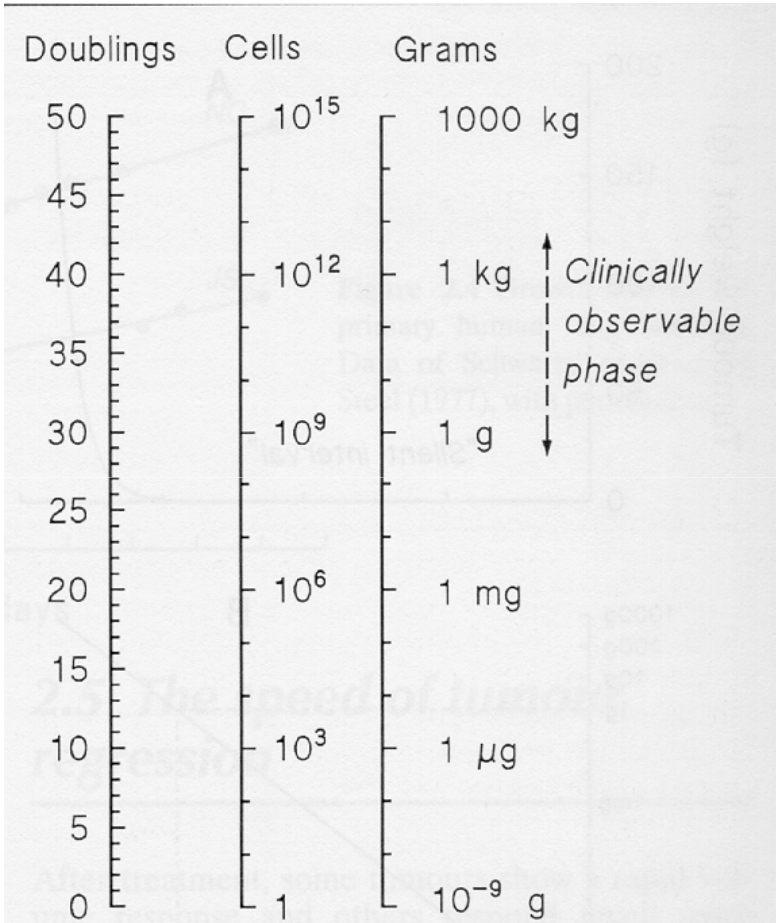

Figure 2.1 The relationship between the weight of a tumour, the number of cells it contains (assuming 10^9 per gram) and the number of doublings from a single cell.

A daganatok növekedése exponenciális

$V = \exp(0{,}693 \times \text{idő} / T_d)$

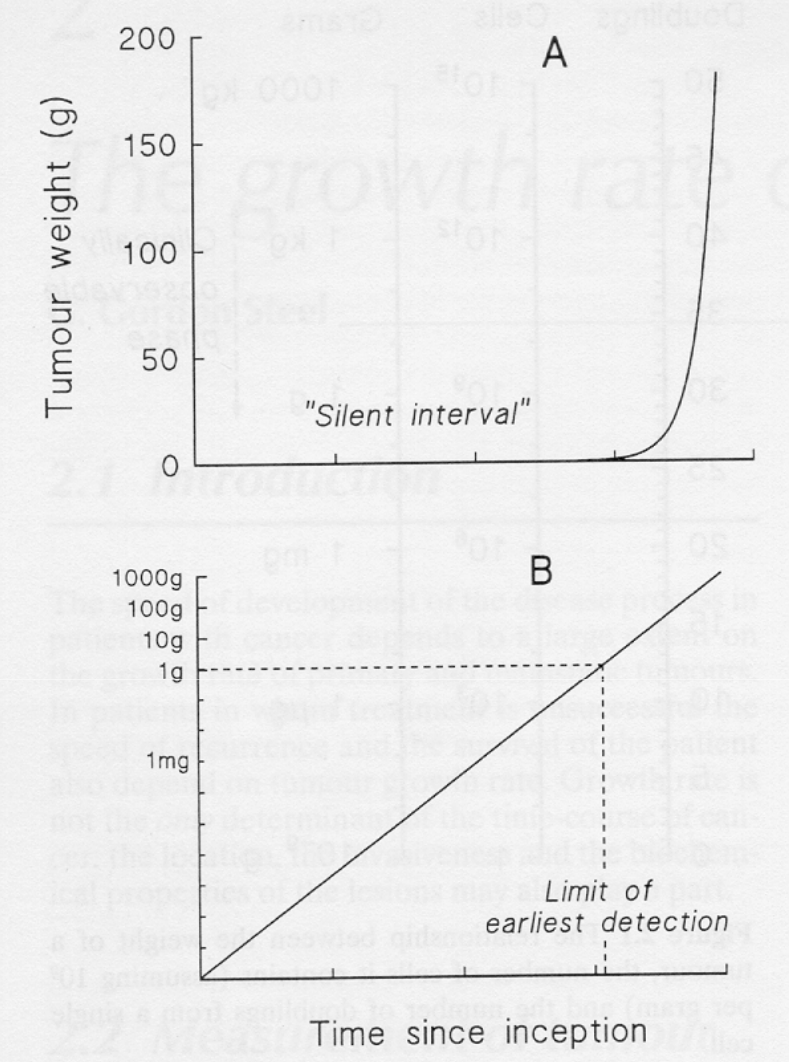

Figure 2.2 An exponential growth curve plotted on a linear scale (**A**) or on a logarithmic scale (**B**). The clinical phase of growth is a minor part of the whole life history of the tumour.

Emberi tumorok növekedése

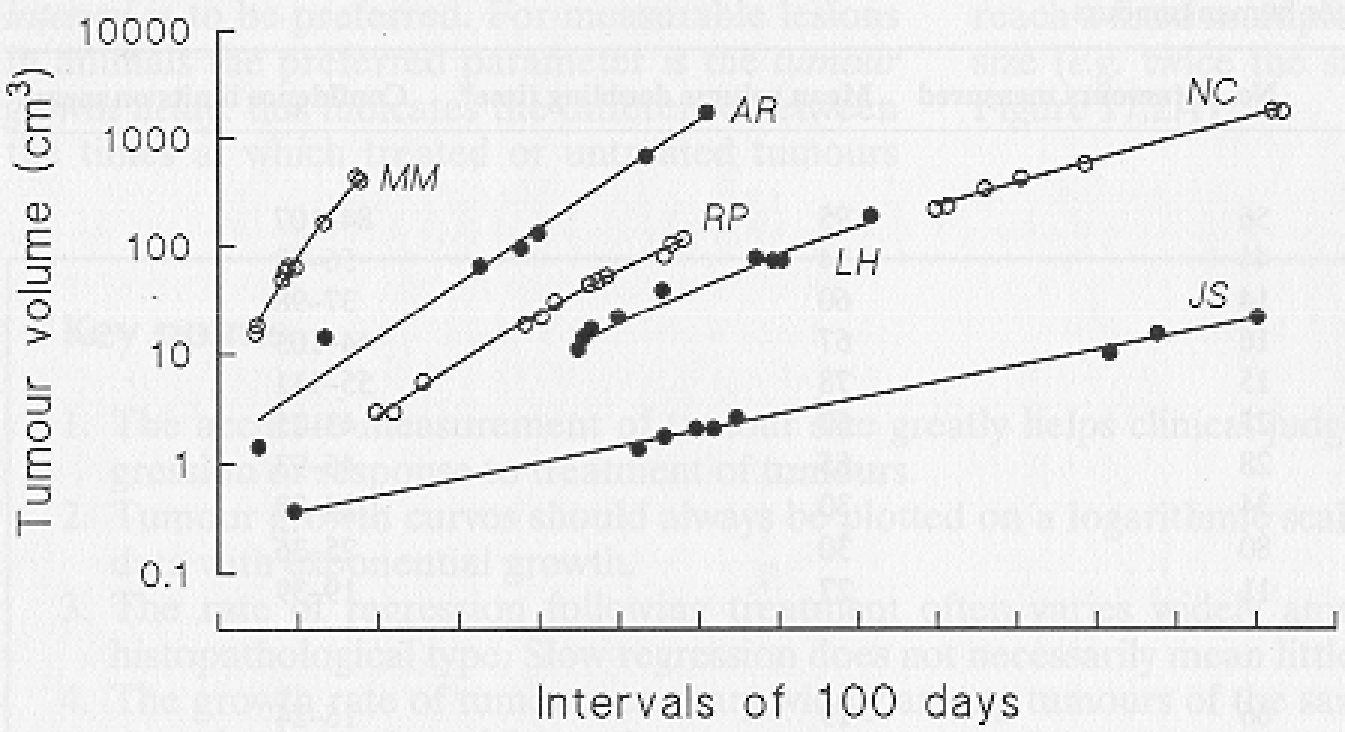

Figure 2.4 Growth curves for primary human lung tumours. Data of Schwartz, redrawn by Steel (1977), with permission.

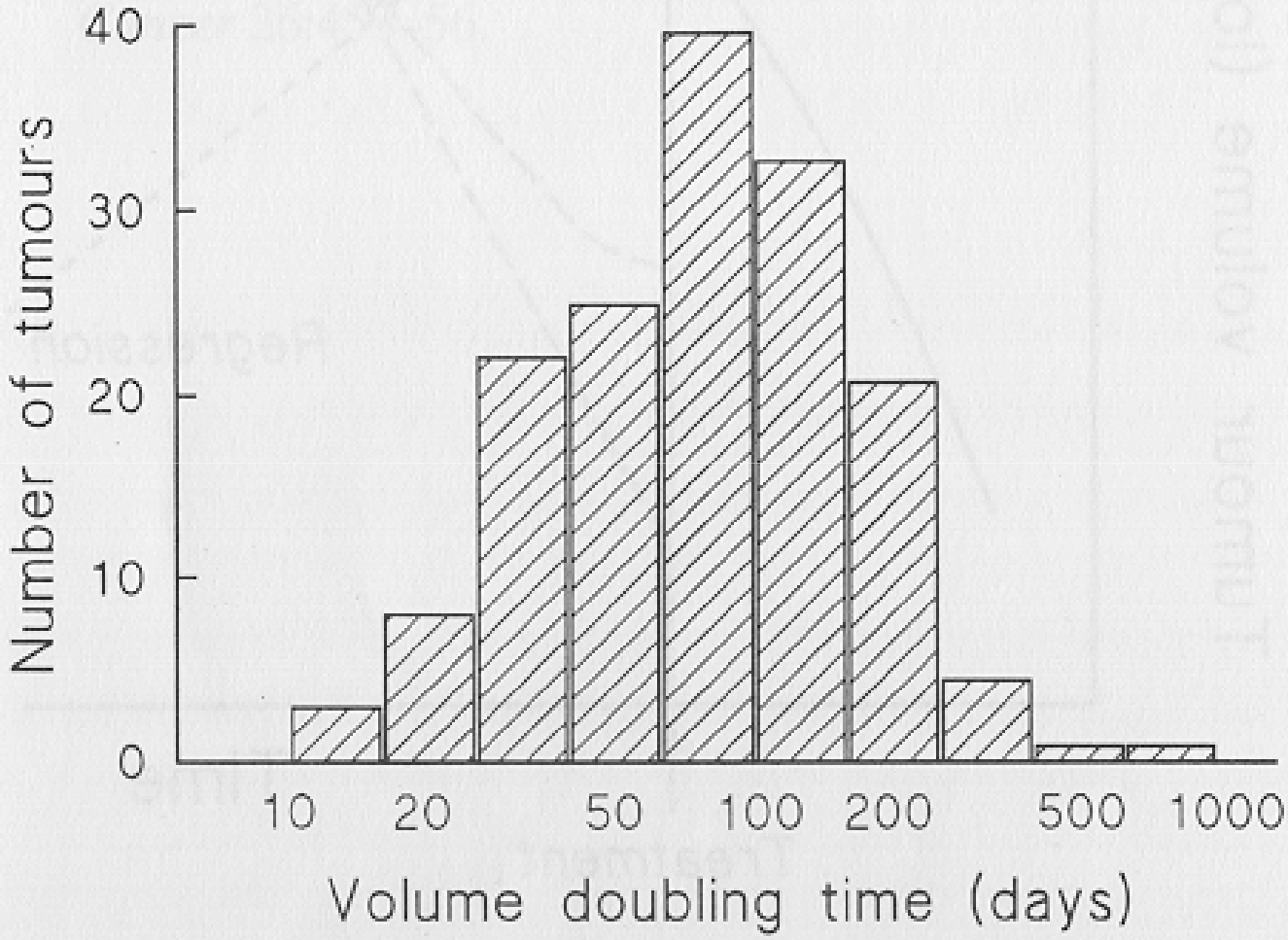

Figure 2.5 The distribution of volume doubling times

Table 2.1 Volume doubling times for human tumours

Site and type	No. of tumours measured	Mean volume doubling time*	Confidence limits on mean
Metastases in lung			
Colon-rectum, adenocarcinoma	56	95	84–107
Breast, adenocarcinoma	44	74	56–98
Kidney, adenocarcinoma	14	60	37–98
Thyroid, adenocarcinoma	16	67	44–103
Uterus, adenocarcinoma	15	78	55–111
Head & neck, sq. cell carcinoma	27	57	43–75
Fibrosarcoma	28	65	46–93
Osteosarcoma	34	30	24–38
Teratoma	80	30	25–36
Lymphoma	11	27	19–39
Superficial metastases			
Breast carcinoma	66	19	16–24
Primary tumours			
Lung, adenocarcinoma	64	148	121–181
Lung, sq. cell carcinoma	85	85	75–95
Lung, undifferentiated	55	79	67–93
Colon-rectum	19	632	426–938
Breast	17	96	68–134

* Geometric mean volume doubling time in days.

From a review of early data on the growth rate of human tumours (Steel, 1977).

Tumor regresszió sugárterápiát követően

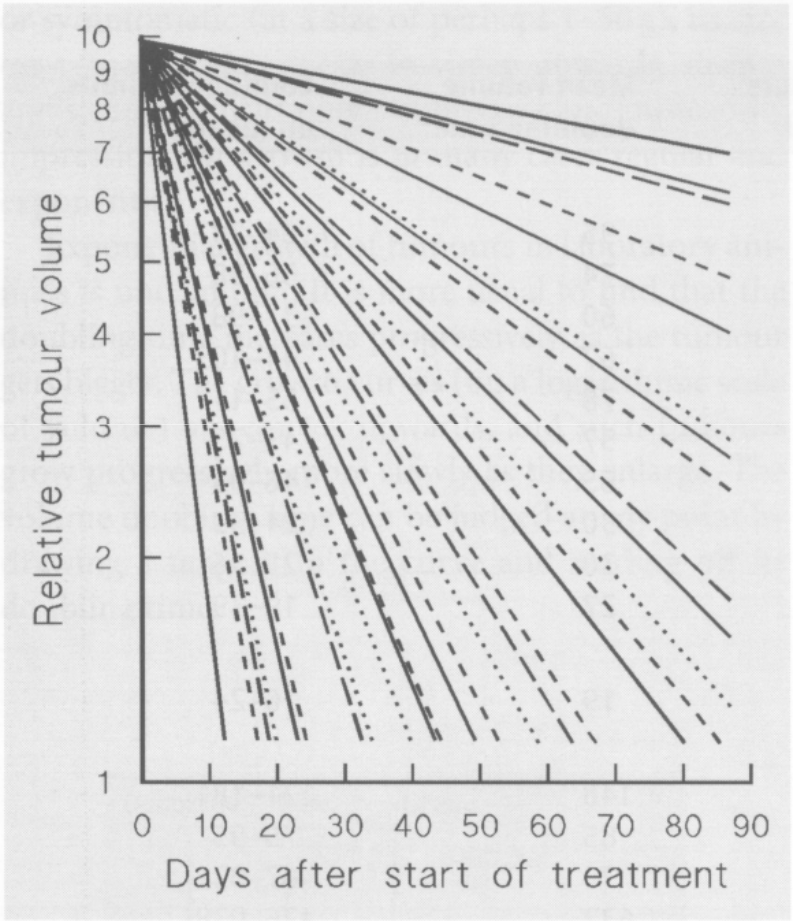

Figure 2.5 *The range of regression rates of some of the 78 primary human breast tumours studied by Thomlinson (1982).*

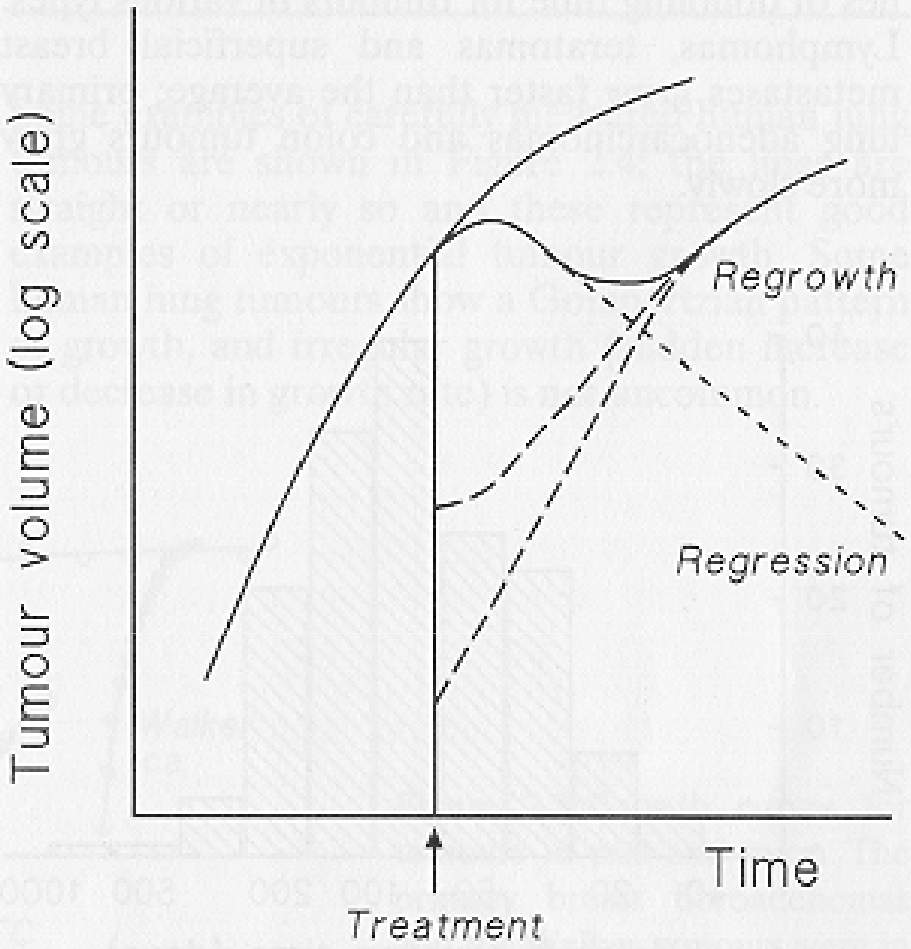

Figure 2.7 The volume response of an uncontrolled tumour is the resultant of two processes: regression and regrowth. Repopulation during the period of regression may take place at a rate that may differ from the growth rate of the untreated tumour.

Valós tumor növekedés

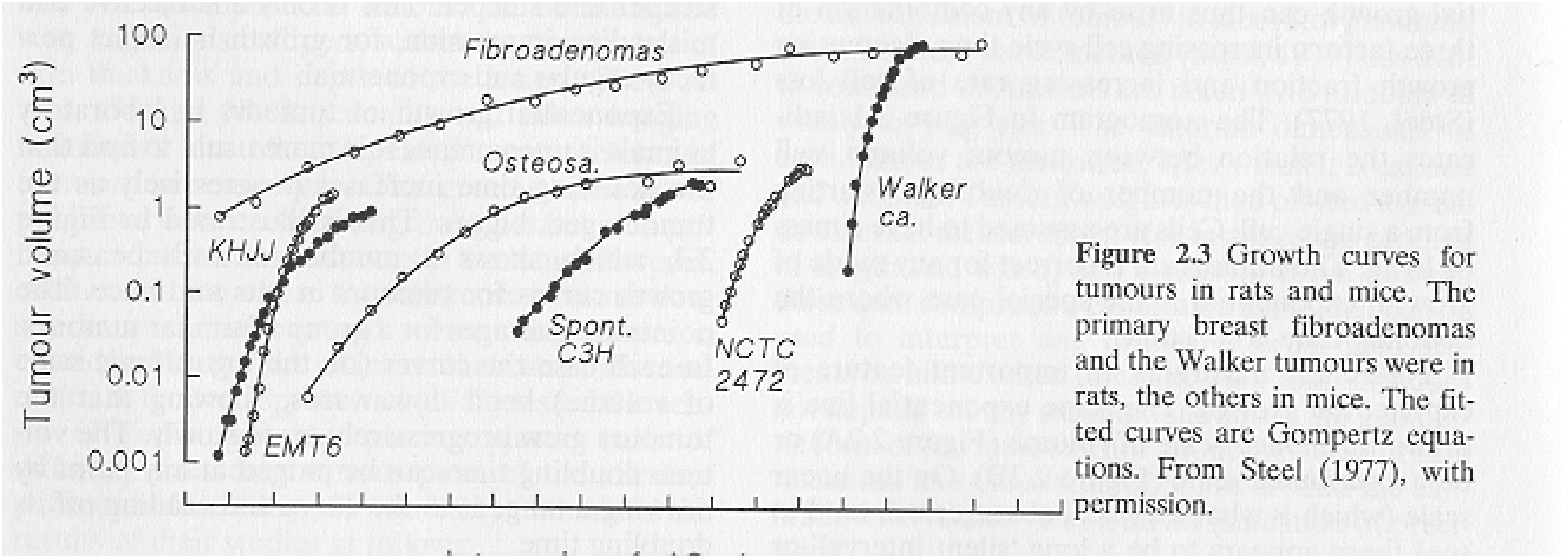

Figure 2.3 Growth curves for tumours in rats and mice. The primary breast fibroadenomas and the Walker tumours were in rats, the others in mice. The fitted curves are Gompertz equations. From Steel (1977), with permission.

Intervals of 100 days

A daganat összetétele

Osztódó sejtek (P)
Nyugalmi állapotú sejtek (G_0)
Differenciálódott sejtek
Sztróma

A daganat növekedését befolyásoló tényezők

A sejtciklus ideje (T_C)

A növekedési frakció (GF)

A sejt veszteség (Φ)

A sejtciklus ideje

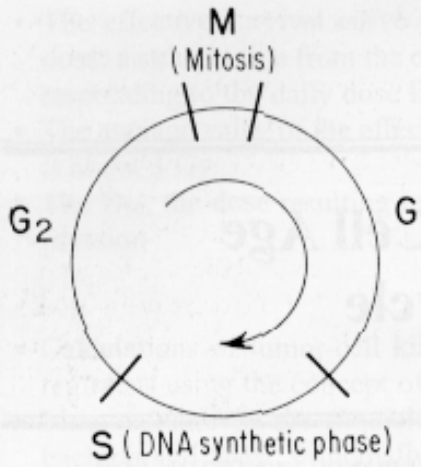

Figure 4.1. The stages of the mitotic cycle for actively growing mammalian cells. M, mitosis; S, DNA synthetic phase; G_1 and G_2, "gaps" or periods of apparent inactivity between the major discernible events in the cycle.

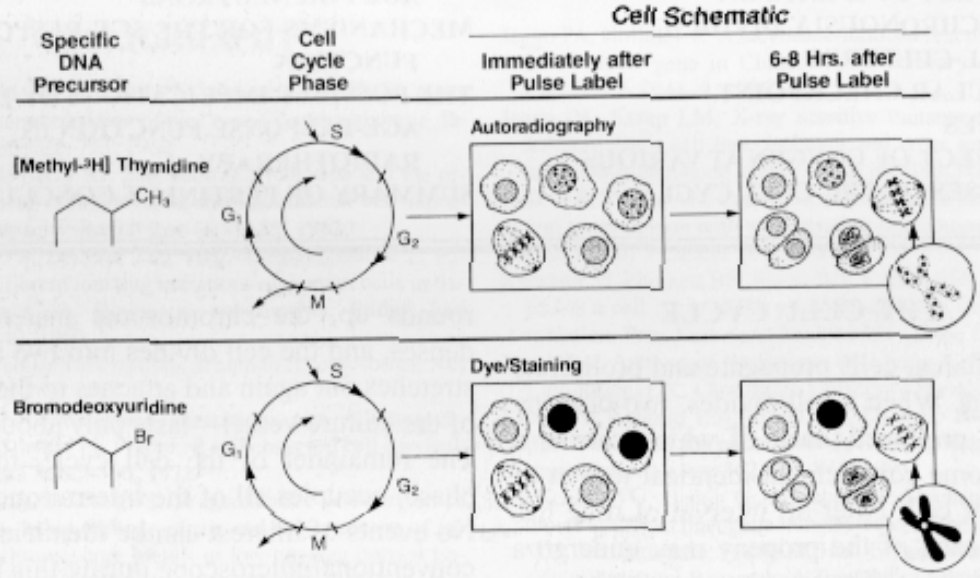

Mitotikus index: a sejtek hányadrésze van a mitózis fázisban

$MI = \lambda T_M / T_C$

Labelling index: a sejtek hányadrésze van S fázisban.

$LI = \lambda T_S / T_C$

Percent labeled mitosis

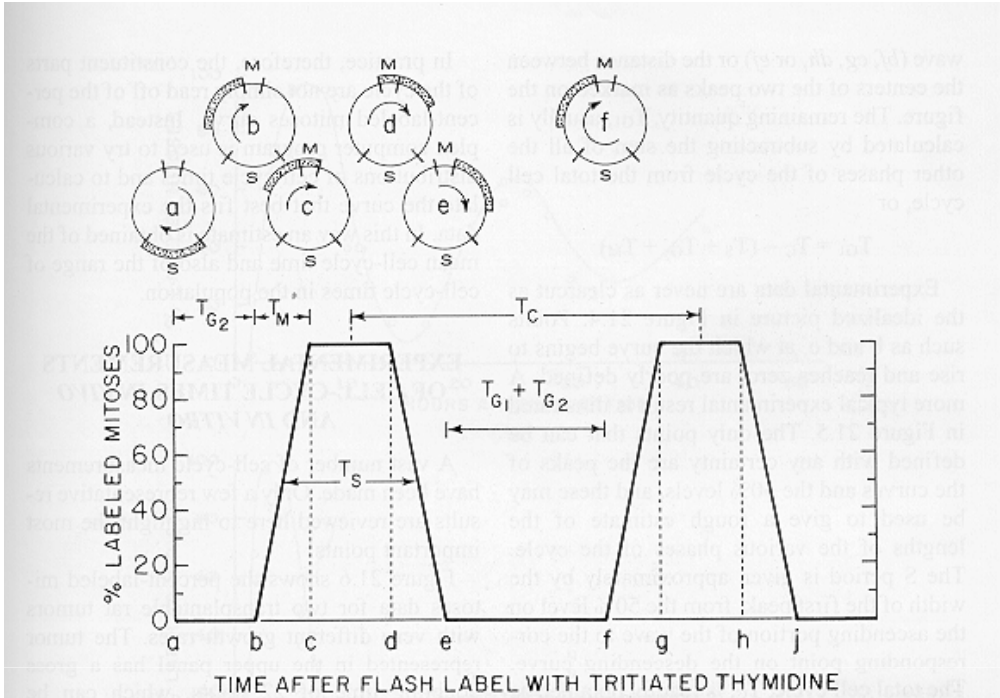

Figure 21.4. Percent-labeled mitoses curve for an idealized cell population in which all of the cells have identical mitotic cycle times. The cell population is flash-labeled with tritiated thymidine, which labels all cells in S. The proportion of labeled mitotic cells is counted as a function of time after labeling. The circles at the top of the figure indicate the position of the labeled cohort of cells as it progresses through the cycle. The length of the various phases (*e.g.*, T_{G2}, T_M) of the cycle (T_C) may be determined as indicated.

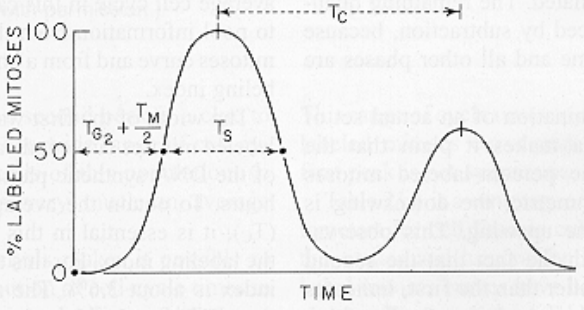

Figure 21.5. Typical percent-labeled mitoses curve obtained in practice for the cells of a tissue or tumor. It differs from the idealized curve in Figure 21.4 in that the only points that can be identified with precision are the peaks of the curve and the 50% levels. The first peak is symmetric, and the second peak is lower than the first because the cells of a population have a range of cell cycle times.

Sejtciklus idő: $T_C = \lambda x T_S / LI$

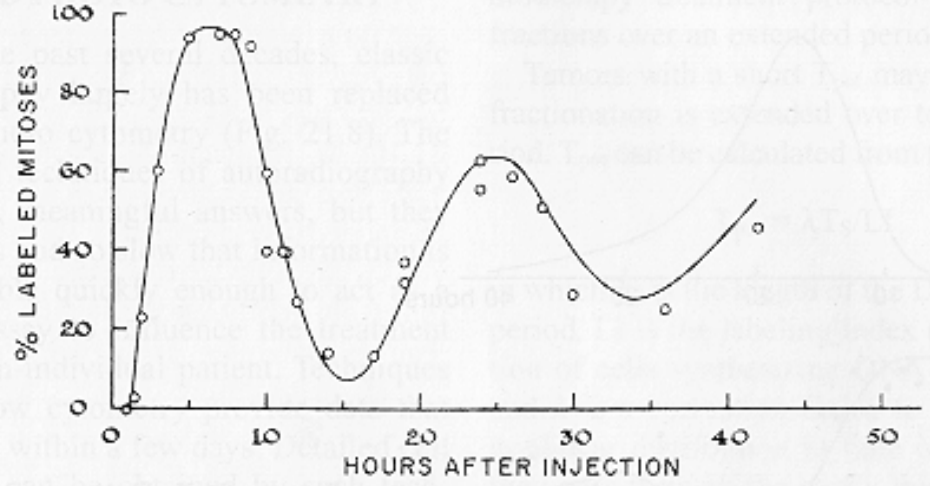

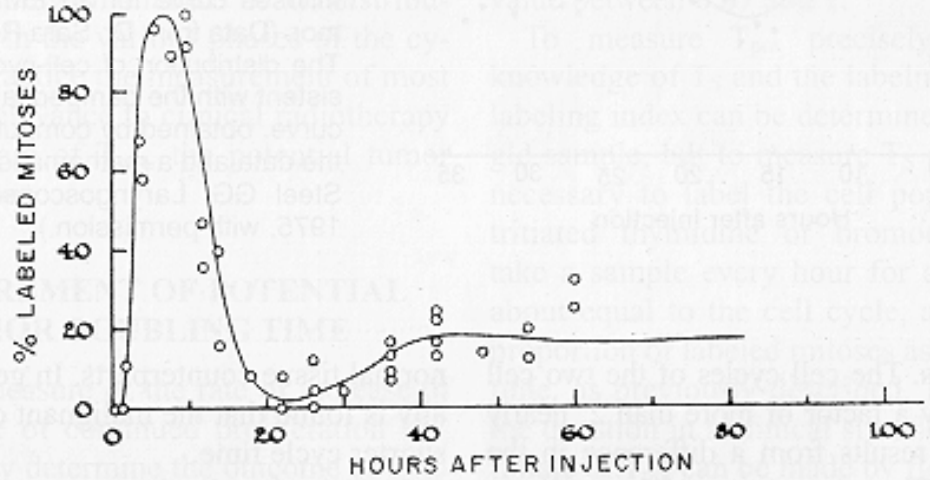

Figure 21.6. Percent-labeled mitoses curve for two transplantable rat sarcomas with widely different growth rates. The tumor in the **upper panel** has a gross doubling time of 22 hours, compared with 190 hours for the tumor in the **lower panel**. (From Steel GG, Adams K, Barratt JC: Analysis of the cell population kinetics of transplanted tumours of widely differing growth rate. Br J Cancer 20:784–800, 1966, with permission.)

TABLE 21.5. *Individual Values for the Duration of the Cell Cycle (T_C) in 41 Human and Solid Tumors of Various Histologic Types*

Authors	T_C, h
Frindel *et al.* (1968)	97, 51.5, 27.5, 48, 49.8
Bennington (1969)	15.5, 14.9
Young and de Vita (1970)	42, 82, 74
Shirakawa *et al.* (1970)	120, 144
Weinstein and Frost (1970)	217
Terz *et al.* (1971)	44.5, 31, 14, 25.5, 26,
Peckham and Steel (1973)	59
Estevez *et al.* (1972)	37, 30, 48, 30, 38, 96, 48
Terz and Curutchet (1974)[a]	18, 19, 19.2, 120
Malaise *et al.* (unpublished data)[a]	24, 33, 48, 42
Muggia *et al.* (1972)	64
Bresciani *et al.* (1974)	82, 50, 67, 53, 58

[a]Measured by the mean grain count halving time.

From Tubiana M, Malaise E: Growth rate and cell kinetics in human tumors: Some prognostic and therapeutic implications. In Symington T, Carter RL (eds): Scientific Foundations of Oncology, pp 126–136. Chicago, Year Book Medical Publishers, 1976, with permission.

TABLE 21.1. *The Constituent Parts of the Cell Cycle for Some Cells in Culture and Tumors in Experimental Animals*

Authors	Cell or Tissue	T_C, h	T_S, h	T_M, h	T_{G2}	T_{G1}
Bedford	Hamster cells *in vitro*	10	6	1	1	2
	HeLa cells *in vitro*	23	8	1	3	11
Steel	Mammary tumors in the rat					
	BICR/M1	19	8	~1	2	8
	BICR/A2	63	10	~1	2	50
Quastler and Sherman	Mouse intestinal crypt	18.75	7.5	0.5	0.5–1.0	9.5
Brown and Berry	Hamster cheek pouch epithelium	120–152	8.6	1.0	1.9	108–140
	Chemically induced carcinoma in pouch	10.7	5.9	0.4	1.6	2.8

T_{pot} a potenciális térfogat megkettőződési idő

$$T_{pot} = \lambda T_S / LI$$

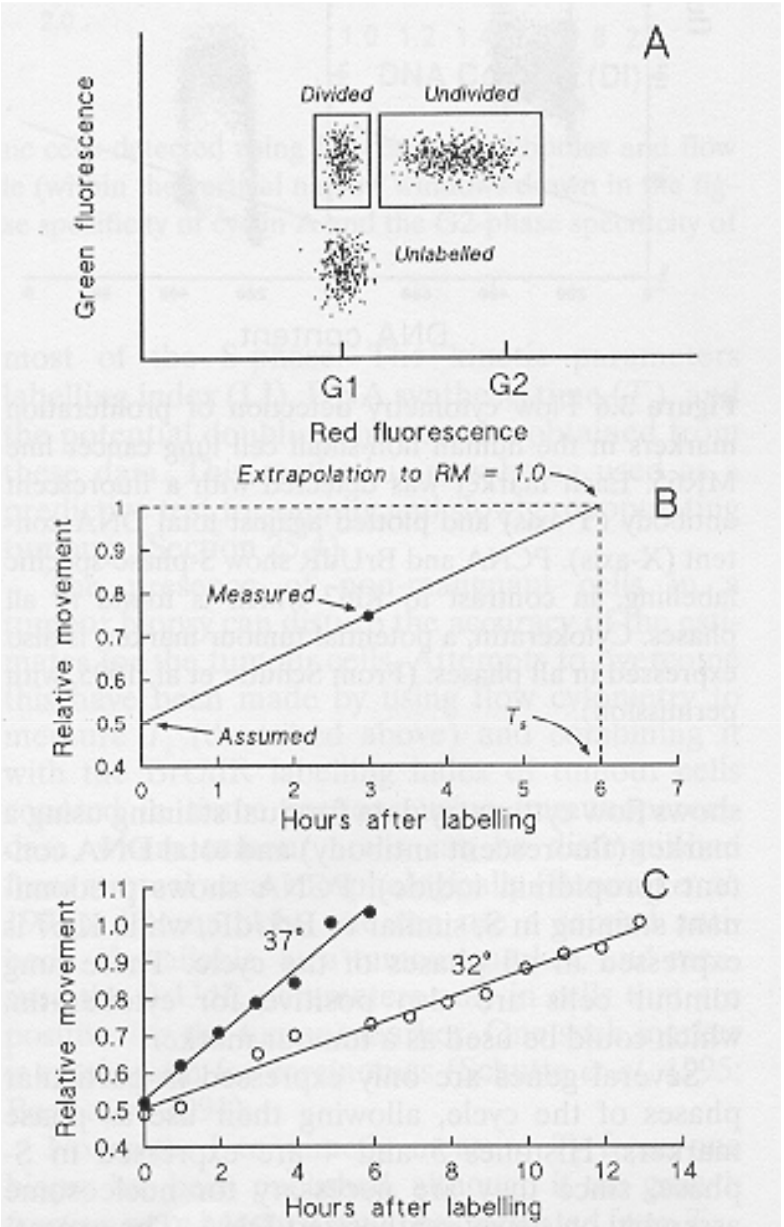

Figure 3.5 Principle of the relative movement method. **A**: the two-dimensional flow-cytometer display; **B**: the principle of the method; **C**: an example of a study on cells at two different temperatures; the difference in slopes indicates different S-phase durations.

Növekedési frakció (GF)

GF = P/P+Q

GF = jelölt mitózisok / jelölt sejtek

TABLE 21.2. *Growth Fraction for Some Tumors in Experimental Animals*

Tumor	Author	Growth Fraction, %
Primary mammary carcinoma in the mouse (G_3H)	Mendelsohn	35–77
Transplantable sarcoma in the rat (RIB_5)	Denekamp	55
Transplantable sarcoma in the rat (SSO)	Denekamp	47
Transplantable sarcoma in the rat (SSB_1)	Denekamp	39
Mammary carcinoma in the mouse (C_3H)	Denekamp	30
Chemically induced carcinoma in the hamster cheek pouch	Brown	29

A sejt veszteség faktor (Φ)

1. Metasztázis
2. Leszakadás
3. Apoptózis
4. Immunrendszer
5. Sejtpusztulás (oxigén, tápanyag hiány)

$$\Phi = 1 - T_{pot}/T_d$$

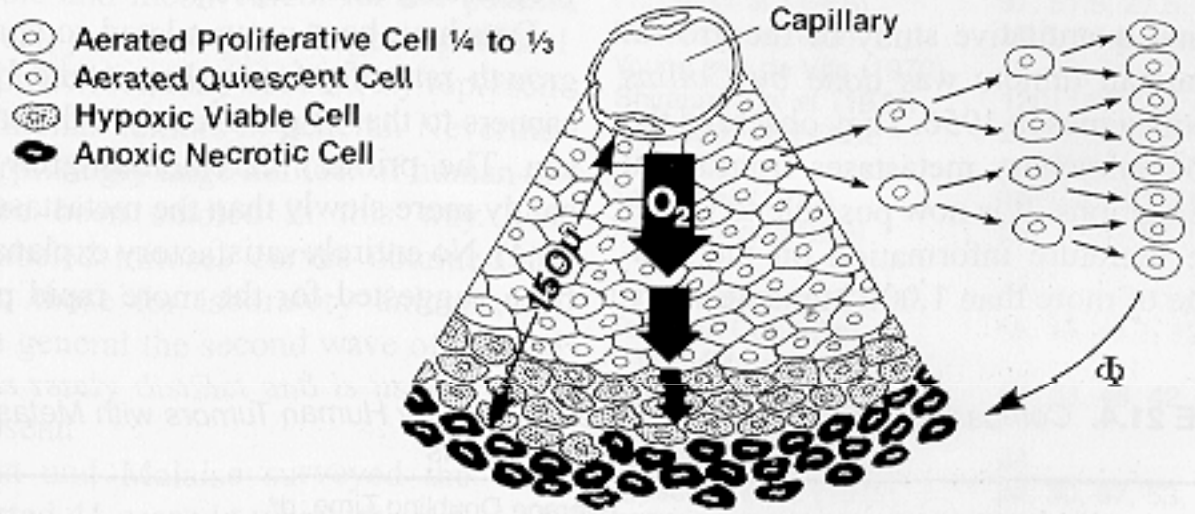

Figure 21.11. The overall pattern of the growth of a tumor. Clonogenic cells consist of proliferative (P) and quiescent (Q) cells. Quiescent cells can be recruited into the cell cycle as the tumor shrinks after treatment with radiation or a cytotoxic drug. In animal tumors the growth fraction is frequently 30 to 50%. Of the cells produced by division, many are lost, principally into necrotic areas of the tumor remote from the vasculature. The cell loss factor (Φ) varies from 0 to 100% and dominates the pattern of tumor growth. As the tumor outgrows its blood supply, some cells become hypoxic. This accounts for some of the quiescent cells that are out of cycle.

TABLE 21.3. *The Cell Loss Factor (Φ) for Some Tumors in Experimental Animals*

Tumor	Author	Φ, %
Mouse sarcoma	Frindel	
3-day-old tumor		0
7-day-old tumor		10
20-day-old tumor		55
Rat carcinoma	Steel	9
Rat sarcoma	Steel	0
Mouse carcinoma	Mendelsohn	69
Hamster carcinoma	Brown	75
Rat sarcoma	Hermens	26
Hamster carcinoma	Reiskin	81–93
Mouse carcinoma	Tannock	70–92

Table 3.2 Cell loss calculations for human tumours

	Thymidine labelling index (%) *(median and range)*	Volume doubling time (days) *(median and range)*	T_{pot} (days)	Cell loss factor (%)
Colorectal carcinoma	15 (10 – 22)	90 (60 – 170)	3.1	96
Squamous cell carcinoma of head and neck	6.9 (5 – 17)	45 (33 – 150)	6.8	85
Undifferentiated bronchial carcinoma	19 (8 – 23)	90 (40 – 160)	2.5	97
Melanoma	3.3	52 (20 – 150)	14	73
Sarcoma	2.0 (0.3 – 6)	39 (16 – 78)	23	40
Lymphoma	3.0 (0.4 – 13)	22 (15 – 70)	16	29
Childhood tumours	13 (10 – 25)	20	3.6	82

From Steel (1977).

Table 2.4 *Calculation of cell loss factors for human tumours based on labelling with radiolabelled thymidine or thymidine analogues and volume doubling times, in separate series*

Site	LI (%)	T_{pot} (d)	T_d (d)	Cell loss factor (%)
(A) Br/IdUrd[1]				
Head and neck	9.6	4.1	45	91
Colorectal	13.1	3.9	90	96
Melanoma	4.2	8.5	52	84
Breast[2]	3.7	9.4	82	89
Prostate[3]	1.4	28.0	1100	97
(B) [^{3}H]Thymidine[4]				
Undifferentiated bronchus ca	19.0	2.5	90	97
Sarcoma	2.0	23.3	39	40
Childhood tumours	13.0	3.6	20	82
Lymphoma	3.0	15.6	22	29

[1] LI, T_s and T_{pot} from FCM data (Haustermans *et al.*, 1997; Rew and Wilson, 2000); calculations assume $\lambda = 0.8$ (Steel, 1977).

[2] T_d values for pulmonary metastases from Spratt *et al.* (1999).

[3] T_d from PSA doubling times; Schmid *et al.* (1993); Fowler *et al.* (1994); Lee *et al.* (1995).

[4] From Steel (1977); calculations assume $T_s = 14$ h, $\lambda = 0.8$.

3.3 Values for kinetic parameters in human tumours

Studies have been carried out in which ^{3}H-thymidine was given to patients and multiple biopsies

Table 3.1 Kinetic parameters of a typical human tumour

Cell cycle time (~2 d)	Potential doubling time (~5 d)	Volume doubling time (~60 d)
Growth fraction (~40%)		
Cell loss (~90%)		

Emberi daganatok növekedése kinetikája

TABLE 21.6. *Volume-Doubling Times of Human Tumors*

Authors	Site	Volume-doubling Time, d	Range, d
Breuer	Lung metastases	40	4–745
Collins *et al.*	Lung metastases	40	11–164
Collins	Lung metastases from colon or rectum	96	34–210
Garland	Primary bronchial carcinoma	105	27–480
Schwartz	Primary bronchial carcinomas	62	17–200
Spratt	Primary skeletal sarcomas	75	21–366

Based on data from Steel GG: Cell loss from experimental tumours. Cell Tissue Kinet 1:193–207, 1968.

TABLE 21.4. *Comparison of the Doubling Times of Primary Human Tumors with Metastases in the Same Individuals*

Histologic Type	Average Doubling Time, d[a]	
	Primary Tumors	Lung Metastases
Squamous cell carcinomas	81.8 (97)	58.0 (51)
Adenocarcinomas	166.3 (34)	82.7 (134)

[a]Number of patients in parentheses.
From Charbit A, Malaise E, Tubiana M: Eur J Cancer 7:307, 1971, with permission.

Nem-radioaktív mérési eljárások

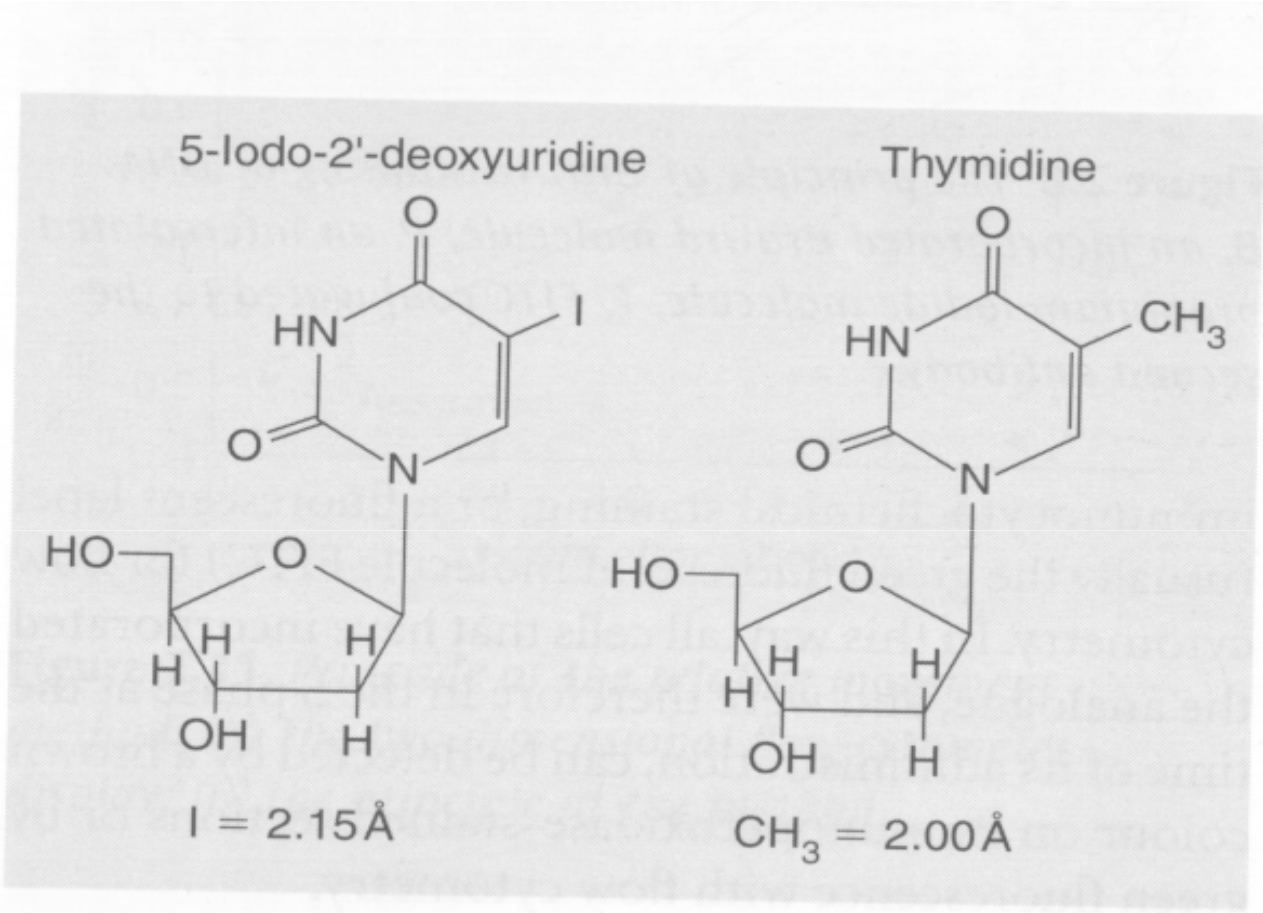

Figure 2.7 *The structure of thymidine and its analogue, IdUrd. The comparative diameters of the iodine atom and the methyl group are indicated.*

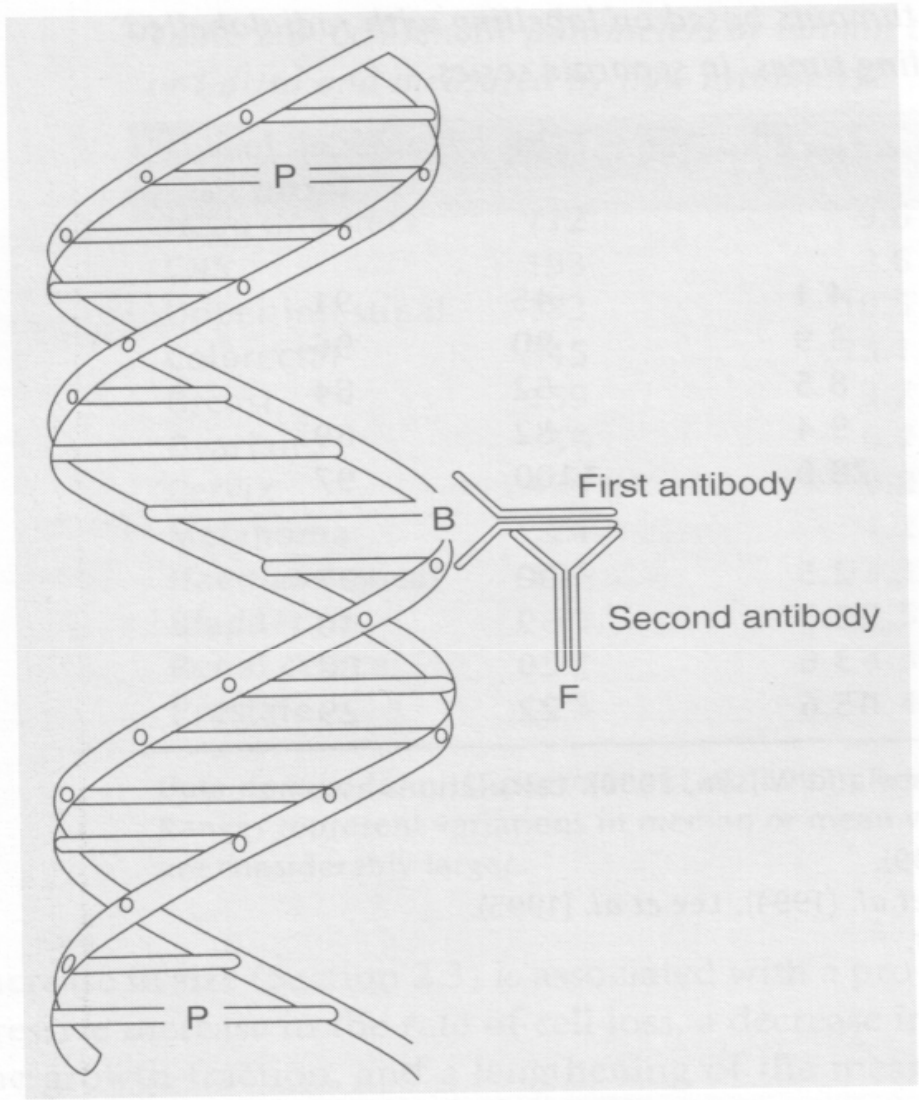

Figure 2.8 *The principle of BrdUrd staining of DNA. B, an incorporated BrdUrd molecule; P, an intercalated propidium iodide molecule; F, FITC conjugated to the second antibody.*

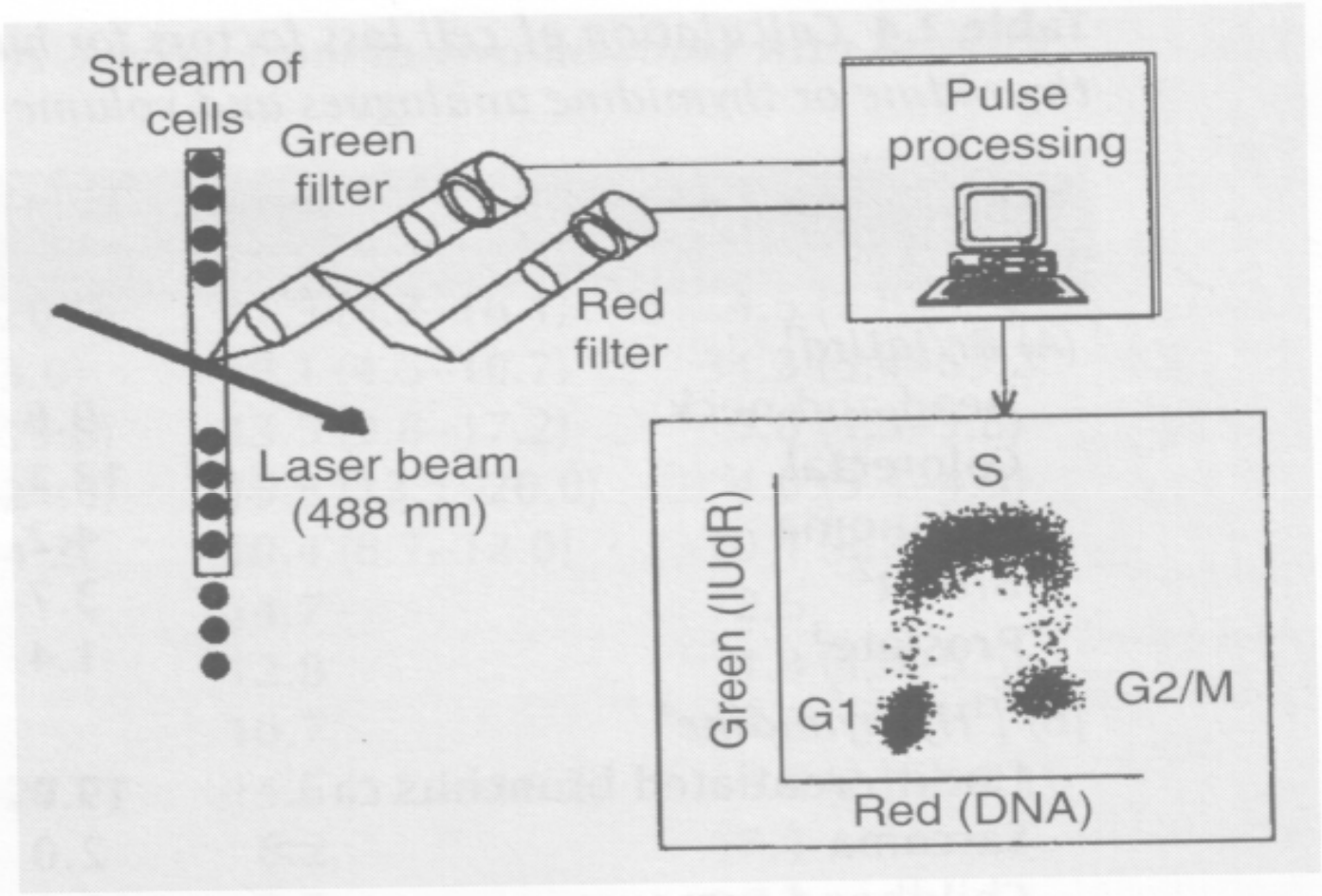

Figure 2.9 *The principle of flow cytometry.*

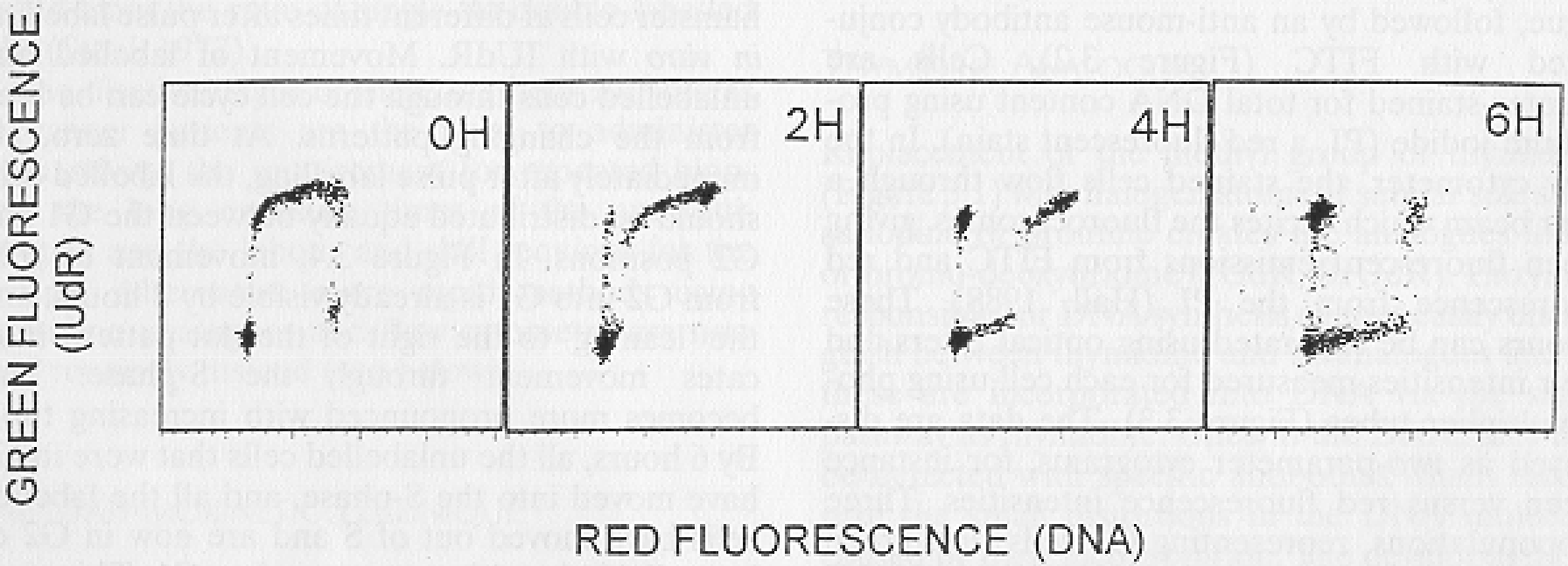

Figure 3.4 Flow cytometer traces from samples taken at various intervals from an *in vitro* cell population that was pulse labelled with IUdR at time zero. Green fluorescence (IUdR content) is plotted vertically; red fluorescence (DNA content) horizontally.

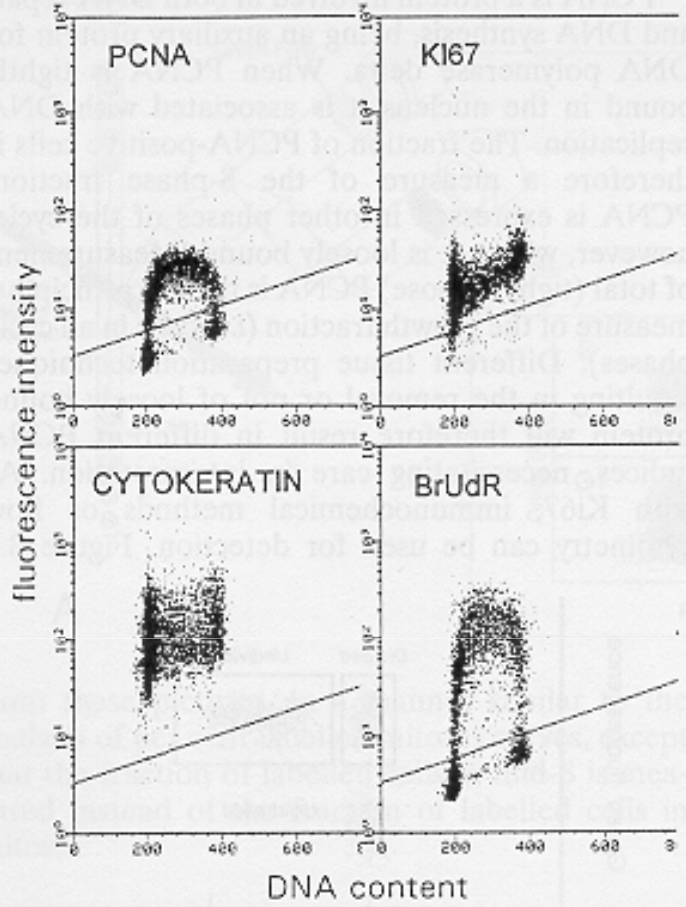

Figure 3.6 Flow cytometry detection of proliferation markers in the human non-small cell lung cancer line MR65. Each marker was detected with a fluorescent antibody (Y-axis) and plotted against total DNA content (X-axis). PCNA and BrUdR show S-phase-specific labelling, in contrast to Ki67 which is found in all phases. Cytokeratin, a potential tumour marker, is also expressed in all phases. (From Schutte et al, 1995, with permission).

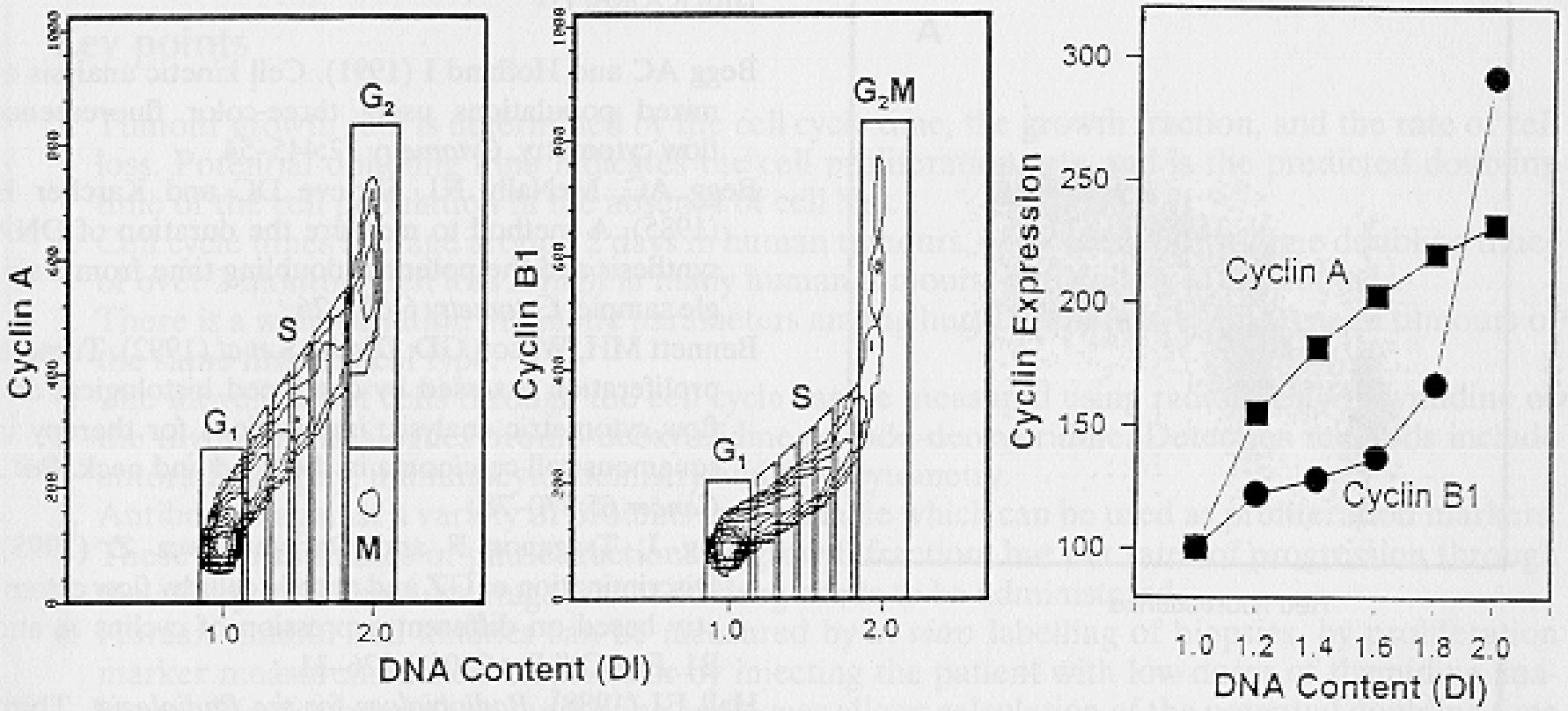

Figure 3.7 Cyclin A and B expression in MOLT4 leukaemic cells detected using fluorescent antibodies and flow cytometry. Cyclin fluorescence in different phases of the cycle (within the vertical narrow windows drawn in the figures) was plotted in the right-hand panel, showing the S-phase specificity of cyclin A and the G2-phase specificity of cyclin B. (From Gong et al, 1995, with permission).

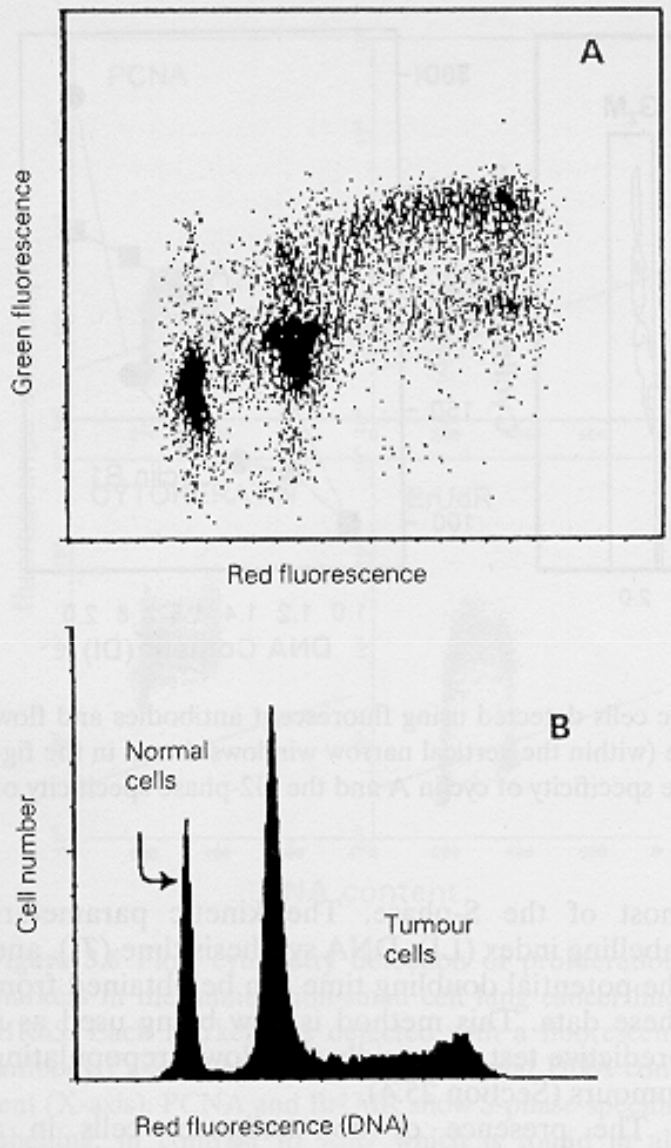

Figure 3.8 Flow cytometry output from a human lung tumour biopsy a few hours after labelling with IUdR. **A**: the two-dimensional display of red-green fluorescence; **B**: the derived distribution of DNA contents.

Table 2.3 *Cell kinetic parameters of human tumours derived from* in vivo *labelling with Br-dUrd or I-dUrd and measured by flow cytometry*

Site	No. of patients	LI (%)	T_s (h)	T_{pot} (d)
Head and neck	712	9.6 (6.8–20.0)	11.9 (8.8–16.1)	4.5 (1.8–5.9)
CNS	193	2.6 (2.1–3.0)	10.1 (4.5–16.7)	34.3 (5.4–63.2)
Upper intestinal	183	10.5 (4.9–19.0)	13.5 (9.8–17.2)	5.8 (4.3–9.8)
Colorectal	345	13.1 (9.0–21.0)	15.3 (13.1–20.0)	4.0 (3.3–4.5)
Breast	159	3.7 (3.2–4.2)	10.4 (8.7–12.0)	10.4 (8.2–12.5)
Ovarian	55	6.7	14.7	12.5
Cervix	159	9.8	12.8	4.8 (4.0–5.5)
Melanoma	24	4.2	10.7	7.2
Haematological	106	13.3 (6.1–27.7)	14.6 (12.1–16.2)	9.6 (2.3–18.1)
Bladder	19	2.5	6.2	17.1
Renal cell ca	2	4.3	9.5	11.3
Prostate	5	1.4	11.7	28.0

Data derived from Haustermans *et al.* (1997); Rew and Wilson (2000).
Ranges represent variations in median or mean values between studies; ranges for individual tumours are considerably larger.

Összefoglalás

- A tumor növekedés nyomon követése elősegíti a daganat progresszió, valamint a kezelésre adott válasz megítélését.
- A tumor növekedés exponenciális, a tumor-térfogat megkettőződési idő több hónap lehet
- A daganat növekedését a sejtciklus idő, a növekedési frakció, valamint a sejtveszteség befolyásolja.
- A sejtciklus idő jelentősen rövidebb a térfogat megkettőződési időnél